OPEN ACCESS Freely available online

Journal of Anesthesia and Clinical Research

Research Article

Imaging Performance of a Handheld Ultrasound System for Thoracic Epidural Analgesia Guidance

Amitabh Gulati[1], Chandni Patel[2], Ajay Patel[3], Jason Chang[3], Rachel Newman[4], Kathryn Ozgun[4], Adam J. Dixon[4*], F. William Mauldin[4]

[1]Department of Anesthesiology and Critical Care Medicine, Memorial Sloan Kettering Cancer Center, New York City, USA;[2]Department of Rehabilitation and Human Performance, Mount Sinai Medical Center, New York City, USA;[3]Department of Rehabilitation Medicine, New York-Presbyterian University Hospital, New York City,USA;[4]Department of Anesthesia, Rivanna Medical, Charlottesville, USA

ABSTRACT

The aim of this study was to evaluate the performance of an ultrasound system with Computer-Aided Detection (CAD) of thoracic spinal landmarks and a thoracic epidural needle guidance algorithm. This study was approved by the institutional review board of the Memorial Sloan Kettering Cancer Center, NY, USA. Algorithm performance was evaluated by imaging the thoracic spines of 55 adult volunteers presenting for pain therapy unrelated to the thoracic spine. The accuracy of the CAD for neuraxial landmark detection was assessed by comparing automated measurements of the lamina depth and midline position to ground-truth annotations provided by physician reviewers. The sensitivity and specificity of the needle guidance algorithm was measured by reviewing the proposed needle trajectory in 435 images. The CAD algorithm detected the lamina depth with an error of 2 mm (95% CI, 1.79-2.39 mm). The spinal midline was detected with an error of 0.5 mm (95% CI, 0.32-0.69 mm). The needle guidance algorithm yielded a sensitivity of 92.4% (95% CI, 90.2%-94.6%) and a specificity of 89.7% (95% CI, 86.3%-93.2%). The results of this study demonstrate the feasibility of computer-aided interpretation for ultrasound imaging of the thoracic spine and for guidance of epidural needle insertion.

Keywords: Thoracic epidural analgesia; Ultrasound; Computer-aided detection; Needle guidance; Anatomical landmarks; Bone-specific imaging

INTRODUCTION

Thoracic Epidural Analgesia (TEA) is an established technique for perioperative pain management following thoracic and abdominal surgical procedures [1]. TEA is administered by placing a catheter within the thoracic epidural space and targeting the infusate to thoracic nerve roots that innervate the injured anatomy. The thoracic epidural space is most commonly accessed percutaneously, with the needle puncture site determined by palpation of surface anatomical landmarks and needle entry to the epidural space confirmed by the loss-of-resistance technique. However, palpation of surface anatomical landmarks is not always reliable for accurate identification of the underlying spinal anatomy, especially in the context of obese or elderly patients with challenging anatomy [2,3]. As a result, TEA administration is associated with a relatively high failure rate (10%-32%) [4-6].

Clinical evidence increasingly supports the use of ultrasound to augment thoracic epidural administration. Compared to manual palpation, ultrasound guidance improves identification of anatomical landmarks for needle placement [3-9]. Enables real-time observation of needle insertion and trajectory, and improves safety by providing direct visualization of the pleural surface [2-12]. For thoracic epidural placement, the use of ultrasound guidance has been shown to reduce the number of needle punctures, decrease patient discomfort, and improve procedural efficacy [3,7-10].

Despite the clinical utility of ultrasound guidance, widespread adoption has been limited due to the technical difficulty of ultrasound image interpretation. Clinical ultrasound systems are designed for soft-tissue imaging, and bone structures are often difficult to interpret [13]. In the thoracic spine, anatomical assessment is further complicated by the extreme caudad angulation of thoracic spinous processes and by acoustic shadowing from bone

Correspondence to: Adam J. Dixon, Department of Anesthesia, Rivanna Medical, Charlottesville, USA, E-mail: adixon@rivannamedical.com

Received: 24-May-2022, Manuscript No. JACR-22-17631; **Editor assigned:** 26-May-2022, Pre QC No. JACR-22-17631 (PQ); **Reviewed:** 09-June-2022, QC No. JACR-22-17631; **Revised:** 15-June-2022, Manuscript No. JACR-22-17631 (R); **Published:** 24-June-2022, DOI: 10.35248/2155-6148.22.13.1059.

Citation: Gulati A, Patel C, Patel A, Chang J, Newman R, Ozgun K, et al. (2022) Imaging Performance of a Handheld Ultrasound System for Thoracic Epidural Analgesia Guidance. J Anesth Clin Res.13:1059.

[2]. Accordingly, the benefit of ultrasound guidance for epidural placement is the most evident for experienced operators [2,14,15]. Further, real-time monitoring of the epidural needle trajectory *via* ultrasound can be cumbersome, due to the absence of a validated guidance technique [2].

To address the technical limitations associated with ultrasound, computational methods have been proposed that improve visualization of bone and provide assistive detection of neuraxial landmarks [16-19]. These methods reduce the learning curve for ultrasound image assessment by automating the detection and measurement of anatomical features, which can serve as a secondary confirmation to physician assessment. The benefit of computer-assisted ultrasound guidance has been established for a variety of lumbar anesthesia and epidural analgesia procedures [2,20]. In prior work, we demonstrated that automated detection of lumbar spine anatomy for spinal anesthesia administration in obese patients can improve first-insertion success rate up to 26%, increase reported patient satisfaction, and reduce the overall number of needle passes by 38% [21]. However, the benefit of computer-aided ultrasound guidance for thoracic procedures has not been established to-date. In this work, we present the first imaging results for a handheld ultrasound system with a dedicated thoracic imaging mode for neuraxial landmark detection and needle guidance. The ultrasound system leverages bone-specific image processing to improve the conspicuity of vertebral structures. For thoracic imaging, the system employs a Computer-Assisted Detection (CAD) algorithm for real-time localization of key neuraxial landmarks, including the spinal process and thoracic lamina. In addition, the system includes a real-time guidance algorithm that yields a suggested needle trajectory for TEA administration. The objective of this work was to evaluate the accuracy of the CAD algorithm for detection of the neuraxial landmarks in human subjects and to assess the sensitivity and specificity of the needle guidance method. The long term goal of this work is to reduce the technical difficulty of ultrasound-guided TEA and ultimately improve procedural outcomes.

MATERIALS AND METHODS

This study was approved by the Institutional Review Board of the Memorial Sloan Kettering Cancer Centre (IRB #18-169). Patients over 18 years of age presenting for pain therapy were eligible to participate. Patients presented with pain symptoms in non-spinal distributions, for example knee pain. All patients possessed a CT (Computed Tomography) of the chest, abdomen, and pelvis within one year of the image gathering. Study exclusion criteria were anatomical deformity of the spine, surgical treatment of the spine, allergies to ultrasound gel, and difficulty being in a seated position. Written, informed consent was obtained from 62 subjects. The data collected in the study was obtained between July 2018 and July 2019.

Imaging study protocol

Subject demographics (age, weight, sex, and BMI) were collected after consent. Ultrasound data was collected prior to any pain therapies, and the imaging data was not used for clinical care. Subjects were placed in a seated position to simulate positioning during a routine TEA procedure. An attending anesthesiologist (AG) skilled in the use of neuraxial ultrasound acquired multiple cine video datasets of each subject's thoracic spine using the Accuro imaging system (Figure 1). Ultrasound datasets were acquired between the T5 and L5 vertebral levels in the transverse imaging plane. For this study, data collected between T5 and T10 were considered [17]. The thoracic Computer-Aided Detection (CAD) algorithm was not used during raw data acquisition. The imaging data was uploaded to a secure server for retrospective review and analysis [1].

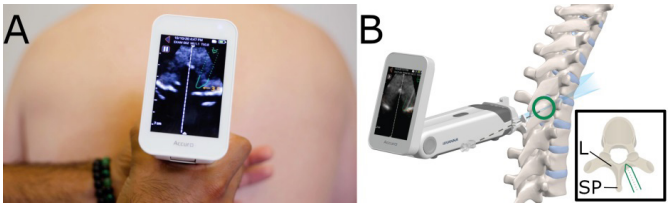

Figure 1: Demonstration of thoracic scanning technique with the Accuro. A. Clinical illustration of device use for thoracic imaging; B. Schematic of the ultrasound beam intersecting the thoracic spine for needle guidance and assessment of the spinous process (SP) and thoracic lamina (L). The green circle depicts the target of needle insertion on the posterior surface of the thoracic lamina. Inset: the preferred paramedian needle placement approach first advances the needle to the posterior surface of the thoracic lamina (green circle) before incremental maneuvering of the needle into the thoracic epidural space.

Bone enhance image reconstruction

The Accuro implemented a real-time bone enhancement algorithm that detected and enhanced the contrast of bone surfaces within the 2D ultrasound images [16,17,19]. Bone surfaces were detected by identifying highly reflective bone surfaces located superficial to regions of dark signal dropout, known as acoustic shadow. The acoustic shadow was detected in real-time by implementing a filter described by the following equation.

Where S (i,j) is the shadow intensity image (Figure 2B), I(k, j) is the B-mode image frame data, α is the depth offset, M is the number of samples in each ultrasound A-line, τ is a small number to avoid division by zero, and wk,I is a depth weighting parameter that accounts for increasing electronic noise through depth that results from time-gain compensation. Bone surfaces (Figure 2C) detected within S (i, j) were recombined with the raw B-mode data to reconstruct the composite bone enhanced image (Figure 2D).

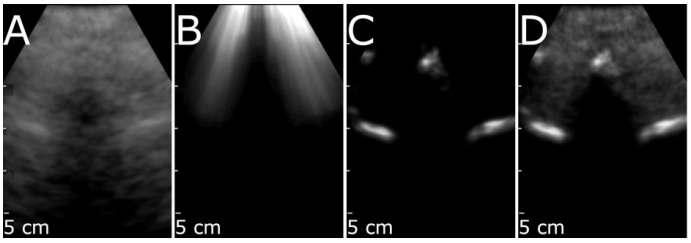

Figure 2: Intermediate images produced by the bone enhancement image processing method. A. Raw B-mode image of thoracic spine; B. Shadow image, S (i, j); C. Intermediate image obtained by dividing the raw image A. by the shadow image B., and scaling by a sigmoid to increase contrast; D. The final thoracic image with enhanced bone signal and suppressed tissue signal.

Thoracic spine CAD algorithm

A subset of high intensity pixels within the bone enhanced images were isolated and served as an input to the thoracic spine CAD algorithm (Figures 3 and 4). The algorithm registers the bone points extracted from individual images against a point-based, 3D model of a thoracic vertebra, using a cost function to maximize the similarity between the observed bone points within the image and the 3D model [19,22]. The cost function utilized in this study

was. Where M is the number of bone points extracted from the bone image, N is the number of points in the 3D model, dist is the Euclidean distance between a model point and an image bone point, and intensity is the brightness of the bone point. In effect, this cost function minimizes the distance between model and image points, while preferentially weighting brighter bone points over dim bone points.

When the value of the cost function was below a pre-defined threshold that defined a good fit between the model and the underlying image data, then graphics were displayed on the Accuro screen to indicate the location of the spine midline and the depth to the thoracic lamina. If the paramedian needle trajectory enforced by the Accuro Locator needle guide intersected with the thoracic lamina, then a green needle trajectory was depicted on the screen to indicate an appropriate needle insertion location that would advance the Tuohy epidural needle to the thoracic lamina surface (Figures 3D and 4D) [1]. The needle trajectory computed by the thoracic CAD algorithm supports a paramedian needle placement approach, as described by Manion [1]. In which the needle is initially advanced to the posterior surface of the thoracic lamina, before being incrementally advanced into the thoracic epidural space.

Neuraxial landmark detection

Three medical residents (CP, AP, and JC) independently identified thoracic anatomical landmarks on individual Bone Enhance images from the cine datasets. In each image, each reviewer manually annotated the location of the spine midline and the location of the thoracic lamina (if present). Representative manual annotations for a single Bone Enhance image of the thoracic spine are depicted in Figure 4B. The reviewers were blinded to the results of the Thoracic Spine CAD algorithm when annotating the images, and each reviewer received training on representative datasets to standardize image annotation techniques. As described in the following Materials, individual images were excluded from follow-on analysis if there was significant disagreement among the reviewers about the location of the anatomical landmarks within the image. The performance of the thoracic spine CAD algorithm was assessed by comparing its automated measurements to the manual annotations provided by the physician reviewers. First, the CAD algorithm used the 3D model-fit to the underlying image data to determine if a thoracic spine cross-section was present in the image. Second, the algorithm determined the location of the spine midline and the thoracic lamina on the basis of a model fit to the extracted bone points, as depicted in Figure 4C. In this study, the accuracy of the measurement and detection of the following anatomical features were assessed: (1) location of the spine midline, (2) depth to the thoracic lamina, and (3) accuracy of needle trajectory localization to the thoracic lamina.

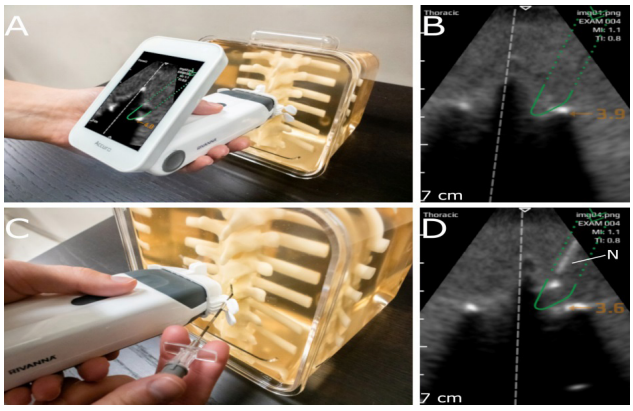

Figure 3: Illustration of the Accuro needle guidance method on a True-View thoracic spine phantom. A. Demonstration of thoracic imaging to visualize spinal anatomy; B. Visualization of suggested needle trajectory to intersect the spinal lamina; C. Demonstration of ultrasound imaging with the needle guide to perform administration of thoracic epidural analgesia; D. Real- time visualization of the needle (N) during needle advancement towards the posterior surface of the thoracic lamina.

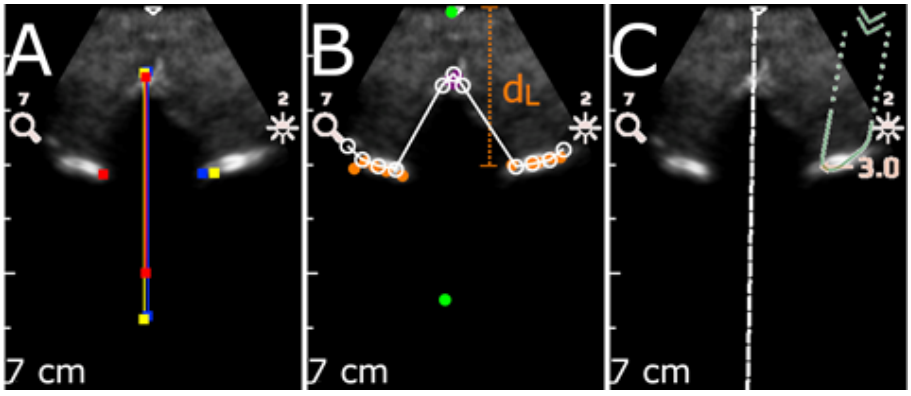

Figure 4: Summary of physician and computer-aided detection (CAD) analysis performed on ultrasound cross-section of the thoracic spine. A. Set of three physician annotations (red, yellow, blue) indicating the midline and lamina depth positions; B. Identification of the lamina (orange), spinous process (purple), and midline boundaries (green) obtained by the Accuro CAD algorithm. The white circles connected by white lines depict a point-representation of a single cross-section of the 3D spine model that is used during the registration process to localize the thoracic anatomy within the image; C. Bone-enhanced image acquired by the Accuro with the midline (white), lamina depth (orange, in cm), and needle trajectory (green) CAD algorithms.

Statistical analysis

The accuracy of the thoracic spine CAD algorithm for lamina depth and midline position was assessed by comparing the CAD measurements to the mean positional annotation from the physician reviewers. A linear regression between the CAD and mean physician annotations was performed to assess measurement correlation. Measurement bias was evaluated using a Bland Altman analysis [23]. The agreements between the CAD and physician measures were determined using the Bland-Altman 95% limits of agreement for the lamina depth and midline, respectively. Sensitivity and specificity of the needle guidance algorithm were measured using the performance classification (Table 1) provided by the independent reviewers as a benchmark. All positional errors and performance measures are expressed as a mean ± standard error. Confidence intervals for all metrics were computed under the assumption of independent, random sampling and Gaussian-distributed random variables. Statistical analysis was performed using Matlab (Mathworks, Natick, MA).

RESULTS

A total of 62 subjects were recruited for the imaging-only study. Data from seven subjects were omitted due to errors or inconsistencies in data acquisition, there by data from 55 subjects were evaluated. The mean subject age was 56.2 ± 13.3 years (range, 24-83 years), with 49.1% of subjects being male. The mean BMI was 29.8, 8.3 kg/m^2 (range, 17.2-54.6 kg/m^2).

Physician annotation

The three physician reviewers each annotated a total of 435 images obtained from the 55 subjects. 27 single annotations and 17 images were excluded from analysis due to physician disagreement (see Materials for data exclusion criteria). A positive tvpeofthe correlation (Pearson r=0.70, 95% CI=[0.65, 0.75]) was found between the mean physician measurements of lamina depth and BMI, and the inter-image standard deviation between physician responses did not increase with BMI (Figure 5). The average lamina depth was 3.75 ± 0.78 cm (range, 1.95-6.51 cm).

Neuraxial landmark detection

The lamina depth and spinal midline measurements estimated by the Accuro were compared with the mean physician annotations for each image. The positional accuracy and classification performance are summarized in Table 2. The CAD estimates of the lamina depth were highly correlated with the physician measurements (Figure 6); Pearson r=0.92, 95% CI=[0.9, 0.93]). Measurement agreement was also confirmed using a Bland-Altman analysis, shown in Figure 6. The upper and lower bounds for the 95% limits of agreement were 0.82 cm and -0.40 cm, respectively. The mean difference (bias) between the physician and CAD measures was 0.21 cm. Similarly, spinal midline CAD estimates were highly correlated with physician measurements (Figure 6; Pearson r=0.89, 95% CI=0.87-0.91). A Bland-Altman analysis for the spinal midline measure is shown in Figure 6, indicating a 0.05 cm mean difference between the physician and CAD measures. The upper and lower bounds for the 95% limits of agreement were 0.43 cm and -0.33 cm.

Needle guidance

The needle trajectory CAD algorithm displayed a suggested needle trajectory for both right and left-handed needle insertion. The needle guidance algorithm yielded a sensitivity of 92.43% (95% CI, 90.2%-94.61%) and a specificity of 89.74% (95% CI, 86.3%-93.16%).Videos of representative real-time needle trajectories are provided in Digital Content 1 and 2.

Digital Content 1 depicts a needle trajectory in a subject with BMI of 38 kg/m^2 , while Digital Content 2 depicts a needle and trajectory in a subject with BMI of 27 kg/m^2. Note that in Digital Content 1, the needle trajectory is only "in!the depicted when the thoracic anatomy is located in the center of the image and the needle trajectory intersects with the surface of the thoracic lamina.

Table 1: Performance classification of the needle trajectory algorithm.

		Reference class	
		+	-
Predicted class	+	True positive Correct depiction of needle trajectory	False positive Incorrect depiction of needle trajectory
	-	False negative Incorrect absence of needle trajectory	True negative Correct absence of needle trajectory

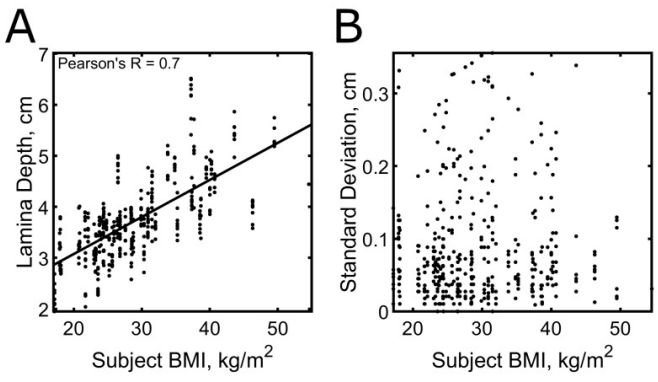

Figure 5: A. The mean annotator lamina depth increases with subject BMI; B. however, the standard deviation of annotator measures was not correlated with BMI, indicating that image quality was sufficient to permit accurate manual annotations across all subjects BMI encountered in the study.

Table 2: Computer-Aided Detection (CAD) algorithm performance metrics.

	Mean	SE	95% CI
Positional error (mm)			
Midline	0.5	0.09	[0.32, 0.69]
Lamina	2.09	0.15	[1.79, 2.39]
Needle trajectory			
Sensitivity (%)	92.4	1.1	[90.3, 94.6]
Specificity (%)	89.7	1.7	[86.3, 93.2]

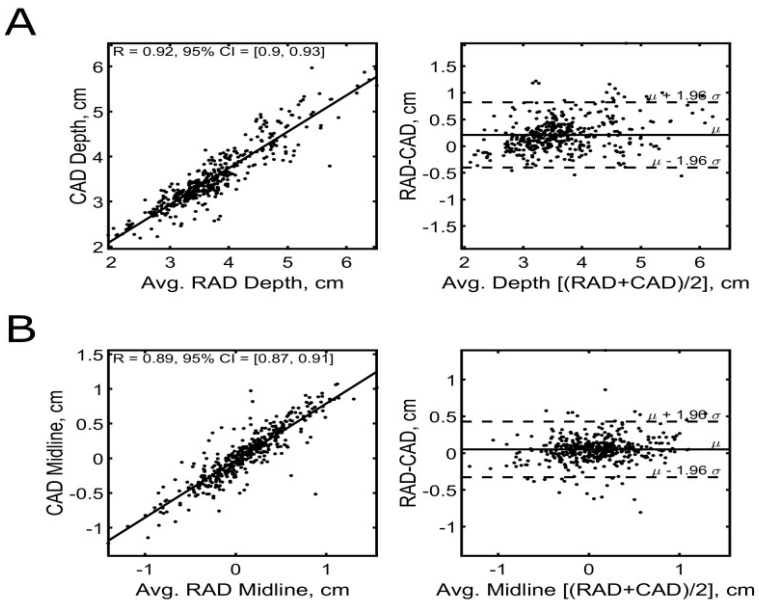

Figure 6: Linear Regression and Bland-Altman plots depicting physician and computer-aided detection (CAD) performance for. **Note:** A. lamina depth B. midline annotations.

Digital Content 1: Demonstration of thoracic imaging with the Accuro for a 38 kg/m BMI subject.The suggested needle trajectory is shown when the thoracic anatomy is located in the center of the image and the needle trajectory intersects with the surface of the thoracic lamina.

Digital Content 2: Demonstration of thoracic imaging with the Accuro for a 27 kg/m BMI subject. The thoracic imaging mode depicts the lamina depth and midline boundary annotations to facilitate rapid and accurate image interpretation.

DISCUSSION

The development of the thoracic Computer Aided Detection (CAD) algorithm was motivated by the understanding that accurate identification of anatomical structures and anticipation of needle trajectories have increased the safety profile and success rates of numerous percutaneous procedures [3,7,10,24-32]. Image guidance has the potential to positively impact the administration of Thoracic Epidural Analgesia (TEA), as blind needle placement in the thoracic epidural space remains one of the most technically challenging interventional procedures, with failure rates exceeding 30% in challenging patients [1,33]. Ultrasound guidance facilitates localization of thoracic anatomy and real-time visualization of needle advancement towards the thoracic epidural space. Indeed, previous randomized controlled trials have demonstrated that perioperative ultrasound examination performed by expert sonographers reduces the number of insertion attempts and decreases the frequency of needle redirection for TEA [3,8]. This study evaluated the performance of an ultrasound methodology developed to provide anatomical landmark localization and needle guidance to the thoracic lamina during TEA procedures. The objective of this work was to establish the agreement between anatomical annotations generated by the CAD algorithm and manual annotations provided by physician reviewers. Overall, a strong correlation was observed between the CAD algorithm and physician annotations of the spinal midline position and lamina depth. The Bland-Altman analysis indicated that the automated detection of the spinal midline and thoracic lamina performed with error on the order of a few millimeters. The CAD-based measurement of the thoracic lamina depth exhibited a consistent underestimation of approximately 2 mm; however, the algorithm was designed to generate conservative lamina depth estimates in order to provide a safety margin for clinicians, as overestimation of the needle puncture depth may lead to wet taps or lung punctures [4,5,34-37]. It should also be noted that underestimation of the depth at which loss of resistance occurs is a frequently reported feature of ultrasound imaging that is most often attributed to tissue compression [17,36]. In addition, we demonstrate preliminary efficacy of an automated needle guidance technology that provides a suggested trajectory for real-time guidance of the Tuohy needle towards the posterior surface of the thoracic lamina. As shown in Table 2, the algorithm demonstrated reliable performance, with an observed sensitivity of 92.4% and specificity of 89.7%. To our knowledge, this is the first demonstration of a real-time needle guidance algorithm that supports the most frequently used percutaneous approach for TEA administration., in which the needle is first advanced to the thoracic lamina before being incrementally maneuvered into the thoracic epidural space [1].The intent of automated landmark localization and needle guidance is to lower the learning curve required to employ ultrasound guidance for TEA administration by providing rapid and accurate image interpretation at the patient bedside. The difficulty of ultrasound image interpretation is a primary barrier to its widespread acceptance [2]. Despite the demonstrated potential to improve procedural efficacy [3,7-9]. By reducing the technical difficulty of ultrasound-guided TEA, this work makes progress toward the long-term goal of improving procedural outcomes. There are limitations to this study.

CONCLUSION

Although the Accuro ultrasound system can acquire ultrasound images in any orientation, the thoracic CAD algorithm only assist with anatomical landmark recognition when imaging transverse plane. Although primary landmarks including the spinous process and thoracic lamina are readily visible *via* transverse scan, the paramedian sagittal view may be more appropriate for localizing the thoracic lamina and entry into the epidural space in Some Cases.Finally,the scope of this study is restricted to an imaging-only analysis , and therefore the impact of thoracic spine CAD technology on clinical care must be further evaluated.

ACKNOWLEDGEMENT

This work was supported by the National Institute of General Medical Sciences of the National Institutes of Health under Award Number R44GM123791. The content is solely the responsibility of the authors and does not necessarily represent the official views of the National Institutes of Health.

DECLARATIONS

K.A.O. and R.M.N. are employees of Rivanna Medical.

F.W.M. and A.J.D. are shareholders of Rivanna Medical and have >5 granted or pending patents that are of relevance to this work.

A.G. made final decisions regarding inclusion of information in this submitted manuscript and has no financial relationship with Rivanna Medical.

REFERENCES

1. Manion SC, BrennanTJ, Riou B. Thoracic epidural analgesia and acute pain management. Anesthesiology. 2011; 115(1): 181-188..
2. Kalagara H, Nair H, Kolli S, Thota G, Uppal, V. Ultrasound imaging of the spine for central neuraxial blockade: A technical description and evidence update. Curr Anesth Rep. 2021; 11(3): 326-339.
3. Hasanin AM, Mokhtar AM, Amin SM, Sayed AA. Preprocedural ultrasound examination versus manual palpation for thoracic epidural catheter insertion. Saudi J Anaesth. 2017;11(1): 62-66.
4. Hermanides J, Hollmann MW, Stevens MF, LirkP. Failed epidural: Causes and management. Br J Anaesth. 2012; 109(2): 144-154.
5. Motamed C, Farhat F, Rémérand F, Stéphanazzi J, Laplanche A. An analysis of postoperative epidural analgesia failure by computed tomography epidurography. Anesth Analg. 2006;103(4): 1026-1032.
6. McLeod GA, Dell K, Smith C, Wildsmith JAW. Measuring the quality of continuous epidural block for abdominal surgery. Br J Anaesth. 2006; 96(5): 633-639.
7. Jadhav KK, Nath G. Ultrasound guided paramedian approach compared with landmark based paramedian approach for thoracic epidural. Ind J Clin Anaesth. 2002;5(1): 75–79.
8. Auyong DB, Hostetter L, Yuan SC, Slee AE, Hanson NA. Evaluation of ultrasound-assisted thoracic epidural placement in patients undergoing upper abdominal and thoracic surgery: A randomized, double-blind study. Reg Anesth Pain Med. 2017;42(2): 204-209.
9. Grau T, Leipold R, Delorme S, Martin E, Motsch J. Ultrasound imaging of the thoracic epidural space. Reg Anesth Pain Med. 2002;27(2):200-206.
10. Pak DJ, Gulati A. Real-time ultrasound-assisted thoracic epidural placement: A feasibility study of a novel technique. Reg Anesth Pain Med. 2018;43(6): 613-615.
11. Marhofer P, Harrop-Griffiths W, Willschke H, Kirchmair L. Fifteen years of ultrasound guidance in regional anaesthesia: Part 2-Recent developments in block techniques. Br J Anaesth. 2010;104(6): 673-683.
12. Luyet C, Eichenberger U, Greif R, Vogt A, Szücs Farkas Z. Ultrasound-guided paravertebral puncture and placement of catheters in human cadavers: An imaging study. Br J Anaesth. 2009;102(4): 534-539.
13. Mauldin FW, Owen K, Tiouririne M, Hossack JA. The effects of transducer geometry on artifacts common to diagnostic bone imaging with conventional medical ultrasound. IEEE Trans Ultrason Ferroelectr Freq Control. 2012;59(6): 1101–1114.
14. Margarido CB, Arzola C, Balki M, Carvalho JCA. Anesthesiologists' learning curves for ultrasound assessment of the lumbar spine. Can J Anaesth. 2010;57(2):120-126.
15. Chin KJ, Perlas A, Chan V, Brown-Shreves D, Koshkin A. Ultrasound imaging facilitates spinal anesthesia in adults with difficult surface anatomic landmarks. Anesthesiology. 2011;115(1): 94-101.
16. Mauldin FW, Owen K, Hossack JA. Three-dimensional spinal bone imaging with medical ultrasound for epidural anesthesia guidance. 2011 IEEE International Ultrasonics Symposium. 2011; 238-241.
17. Tiouririne M, Dixon A J, Mauldin FW, Scalzo D, Krishnaraj A. Imaging performance of a handheld ultrasound system with real-time computer-aided detection of lumbar spine anatomy: A feasibility study. Invest Radiol. 2017;52(8): 447-455.
18. Tran D, Rohling RN. Automatic detection of lumbar anatomy in ultrasound images of human subjects. IEEE Trans Biomed Eng. 2010; 57(9): 2248-2256.
19. Tiouririne M, Nguyen S, Hossack JA, Owen K, William Mauldin F. Handheld real-time volumetric imaging of the spine: Technology development. J Med Eng Technol. 2014;38(2): 100-103.
20. Ghisi D, Tomasi M, Giannone S, Luppi A, Aurini L. A randomized comparison between Accuro and palpation-guided spinal anesthesia for obese patients undergoing orthopedic surgery. Reg Anesth Pain Med. 2019;10(11):100534-100538.
21. Singla P, Dixon AJ, Sheeran JL, Scalzo D, Mauldin FW. Feasibility of spinal anesthesia placement using automated interpretation of lumbar ultrasound images: A prospective randomized controlled trial. J Anesth Clin Res. 2019;10(2): 870-878.
22. Rohr K. Landmark-Based Image Analysis: Using geometric and intensity models. Springer Netherlands. 2001;15(2):102-113.
23. Myles PS, Cui J. Using the Bland–Altman method to measure agreement with repeated measures. Br J Anaesth. 99(3): 309-311.
24. Yeung J H, Gates S, Naidu B V, Wilson MJ, Gao Smith F. Paravertebral block versus thoracic epidural for patients undergoing thoracotomy. Cochrane Database Syst Rev. 2016;63(2): 9090-9121.
25. Teoh DA, Santosham K L, Lydell C C, Smith DF, Beriault MT. Surface anatomy as a guide to vertebral level for thoracic epidural placement. Anesth Analg. 2009;108(5): 1705-1707.
26. Chin KJ, Karmakar MK, Peng P. Ultrasonography of the adult thoracic and lumbar spine for central neuraxial blockade. Anesthesiology. 2011;114(6): 1459-1485.
27. Vallejo MC, Phelps AL, Singh S, Orebaugh SL, Sah N. Ultrasound decreases the failed labor epidural rate in resident trainees. Int J Obstet Anesth. 2010;19(4): 373-378.
28. Bouaziz H, Zetlaoui PJ, Pierre S, Desruennes E, Fritsch N. Guidelines on the use of ultrasound guidance for vascular access. Anaesth Crit Care Pain Med. 2015;34(1): 65-69.
29. Weiner MM, Geldard P, Mittnacht AJC. Ultrasound-guided vascular access: A comprehensive review. J Cardiothorac Vasc Anesth. 2013;27(2):345-360.
30. Bick U, Trimboli R M, Athanasiou A, Balleyguier C, Baltzer PAT. Image-guided breast biopsy and localisation: Recommendations for information to women and referring physicians by the European Society of Breast Imaging. Insights Imaging. 2020;11(1): 12.
31. Ahn SS, Kim E K, Kang DR, Lim SK, Kwak JY. Biopsy of thyroid nodules: Comparison of three sets of guidelines. AJR Am J Roentgenol. 2010;194(1): 31-37.
32. Stoneham MD, Quinlan J. 'Putting the TEA back into teaching': Are trainees being taught optimal epidural techniques? Br J Anaesth. 2015;114(6): 872-874.
33. Kooij FO, Schlack WS, Preckel B, Hollmann M W. Does regional analgesia for major surgery improve outcome? Focus on epidural analgesia. Anesth Analg. 2014;119(3): 740-744.

34. Sessler DI, Standl T, Schroeder F, Bartz HJ, Beyer JC, and Schulte am Esch J. Non-thermoregulatory shivering in patients recovering from isoflurane or desflurane anesthesia. Anesthesiology. 1998; 89 (4): 878-86.

35. Nishiyama T. Thoracic epidural catheterization using ultrasound in obese patients for bariatric surgery. J Res Obes. 2014;15(6):1-6.

36. Baglioni, S., Paolatti, S., Velardo, M. Capogna, G. Accuracy of the SpineNav3DTM ultrasound technology in estimating the epidural space depth for epidural and spinal insertion in pregnant obese patients. OJAnes. 2021;11(8): 221-228.

37. Lee JH, Kim DH, Koh WU. Real-time ultrasound guided thoracic epidural catheterization: A technical review. Anesth Pain Med. 2021;16(4): 322-328.